

See discussions, stats, and author profiles for this publication at: <https://www.researchgate.net/publication/257637273>

Light-dependent and light-independent protochlorophyllide oxidoreductases share similar sequence motifs —in silico studies

ARTICLE in PHOTOSYNTHETICA · DECEMBER 2012

Impact Factor: 1.41 · DOI: 10.1007/s11099-012-0057-z

CITATIONS

4

READS

33

4 AUTHORS, INCLUDING:



[Michał Gabruk](#)

Jagiellonian University

7 PUBLICATIONS 9 CITATIONS

[SEE PROFILE](#)



[Joanna Grzyb](#)

Institute of Physics of the Polish Academy o...

23 PUBLICATIONS 365 CITATIONS

[SEE PROFILE](#)



[Mysliwa-Kurdziel Beata](#)

Jagiellonian University

22 PUBLICATIONS 177 CITATIONS

[SEE PROFILE](#)

Light-dependent and light-independent protochlorophyllide oxidoreductases share similar sequence motifs – *in silico* studies

M. GABRUK^{*}, J. GRZYB^{**}, J. KRUK^{*,+}, and B. MYSLIWA-KURDZIEL^{*}

Department of Plant Physiology and Biochemistry, Faculty of Biochemistry, Biophysics and Biotechnology, Jagiellonian University, ul. Gronostajowa 7, 30-387 Kraków, Poland^{}
Laboratory of Biological Physics, Institute of Physics PAS, al. Lotników 32/46, 02-668 Warsaw, Poland^{**}*

Abstract

In the present studies, we have found a fragment of amino acid sequence, called TFT motif, both in light-dependent protochlorophyllide oxidoreductase (LPOR) and in the L subunit of dark-operative (light-independent) protochlorophyllide oxidoreductases (DPOR). Amino acid residues of this motif shared similar physicochemical properties in both types of the enzymes. In the present paper, physicochemical properties of amino acid residues of this common motif, its spatial arrangement and a possible physiological role are being discussed. This is the first report when similarity between LPOR and DPOR, phylogenetically unrelated, but functionally redundant enzymes, is described.

Additional key words: chlorophyll biosynthesis, homology modeling, protochlorophyllide, protochlorophyllide oxidoreductase, sequence analysis.

Introduction

Reduction of protochlorophyllide (Pchl_{id}) to chlorophyllide (Chl_{id}) is the key step in chlorophyll and bacteriochlorophyll biosynthesis (Fig. 1) (Masuda 2008). As a result of this reaction, one double bond of the Pchl_{id} molecule is reduced and Chl_{id} is formed. Two types of enzymes catalyzing Pchl_{id} reduction exist. In photosynthetic anoxygenic bacteria, only light-independent, dark-operative protochlorophyllide oxidoreductase (DPOR) is found. On the other hand, in angiosperms only a photoenzyme NADPH:Pchl_{id} oxidoreductase (LPOR) occurs and Pchl_{id} to Chl_{id} conversion is strictly light-dependent (Schoefs and Franck 2003). In other photosynthetic organisms both enzymes are present.

It is generally assumed that LPOR and DPOR belong to different enzyme families and have evolved independently. LPOR is a single-chain, nuclear-encoded protein belonging to the family of short chain dehydrogenases/

reductases (SDR) (Yang and Cheng 2004, Reinbothe *et al.* 2010). It shows a regulatory function in angiosperm development, namely in the induction of deetiolation (Schoefs and Franck 2003, Schoefs 2005, Belyaeva and Litvin 2007). LPOR is also in the focus of attention as a model of oxidoreductases (Heyes and Hunter 2005, Sytina *et al.* 2009).

DPOR consists of three protein subunits, which are products of *bchL/chlL*, *bchB/chlB*, and *bchN/chlN* genes, in bacteria/plants. The subunits of DPOR show significant sequence homology with three subunits of nitrogenase (Masuda 2008, Reinbothe *et al.* 2010) catalyzing the formation of ammonia from dinitrogen (Igarashi and Seefeldt 2003). [BchB–BchN]₂ heterotetramer (NB-protein) and [BchL]₂ dimer (L-protein) form the functional DPOR macrodomain and function as the catalytic and reductase components, respectively (Schoefs and Franck 2003, Masuda 2008, Reinbothe *et al.* 2010).

Received 20 January 2012; accepted 7 July 2012.

⁺Corresponding author; fax: 48 12 664 6902; e-mail: jerzy.kruk@uj.edu.pl

Abbreviations: BchB, BchL and BchN – B, L and N subunits of bacterial DPOR, respectively; ChlL – L subunit of plant DPOR, Chl_{id} – chlorophyllide; DPOR – dark-operative (light-independent) protochlorophyllide oxidoreductase; LPOR – light-dependent protochlorophyllide oxidoreductase; NCBI – National Center for Biotechnology Information; NifH – a protomer of Fe protein of nitrogenase; Pchl_{id} – protochlorophyllide; PDB – Protein Data Bank; PORA – one of the isoforms of LPOR; SDR – short chain dehydrogenases/reductases

Acknowledgements: This work was partially supported by grant 2011/01/B/NZ1/00119 from National Center of Science of Poland (NCN). J.G. acknowledges support by the Foundation for Polish Science, Homing Plus Programme co-financed by the European Union within the European Regional Development Fund. The Faculty of Biochemistry, Biophysics and Biotechnology of the Jagiellonian University is a beneficiary of the structural funds from the European Union (grant No: POIG.02.01.00-12-064/08 – “Molecular biotechnology for health”).

Although LPOR and DPOR catalyze the same reaction, these enzymes are completely different as far as their genes, protein structure and catalytic mechanisms are concerned. Bearing in mind a possibility of functional convergence, we have compared currently known sequen-

ces of LPORs and DPORs *in silico* to investigate if there exists any sequence similarity between the enzymes, which could be useful in further analysis of their function.

Materials and methods

Sequence analysis: Several protein sequences of the L, N, and B subunits of DPOR from NCBI (National Center of Biotechnology Information) database (Pruitt *et al.* 2006) were compared to the *Arabidopsis thaliana* PORA sequence (NCBI accession number: NP_200230). Blast algorithm with default parameters set (matrix - Blossum62, penalty for opening the gap - 11, penalty for extending the gap - 1, threshold - 10, word size - 3) was used. Similar fragments between *A. thaliana* PORA sequence and L subunits of DPOR, both BchL and ChlL, have been found. No similarities were found in the case of N and B subunits of DPOR.

Then, a database was constructed by selecting all available sequences of LPOR from green plants and L subunits of DPOR (both BchL and ChlL) from NCBI protein database (status for July 15th, 2011). The database was searched for sequences termed "protochlorophyllide NADPH oxidoreductase" and "L subunit light-independent reductase", for LPOR and DPOR respectively. The hits were manually checked to remove any

mismatched or partial sequences. The following criteria were used: sequences longer than 190 amino acids (1) and predicted involvement in Pchlde reduction (2). The adjusted database finally comprised 42 sequences of LPOR and 117 sequences of BchL/ChlL, fulfilling these criteria (Table 1). The NCBI protein database was searched also to find NADPH-binding SDR proteins and Fe protein of nitrogenases (NifH) that were compared to LPOR and BchL/ChlL, respectively. Then the hits were manually checked again for mismatched or partial sequences. Finally, 270 and 141 sequences of SDR and NifH, respectively, were analyzed.

The sequence alignment was performed using ClustalW (Thompson *et al.* 1994) separately for BchL/ChlL, LPOR, SDR and NifH sequences from the constructed protein sequence database. Default parameter settings were applied, *i.e.* matrix - Gonnet 250, penalty for opening the gap - 10, endgaps - excluded, penalty for extending the gap - 0.2, gap separation penalty - 4.

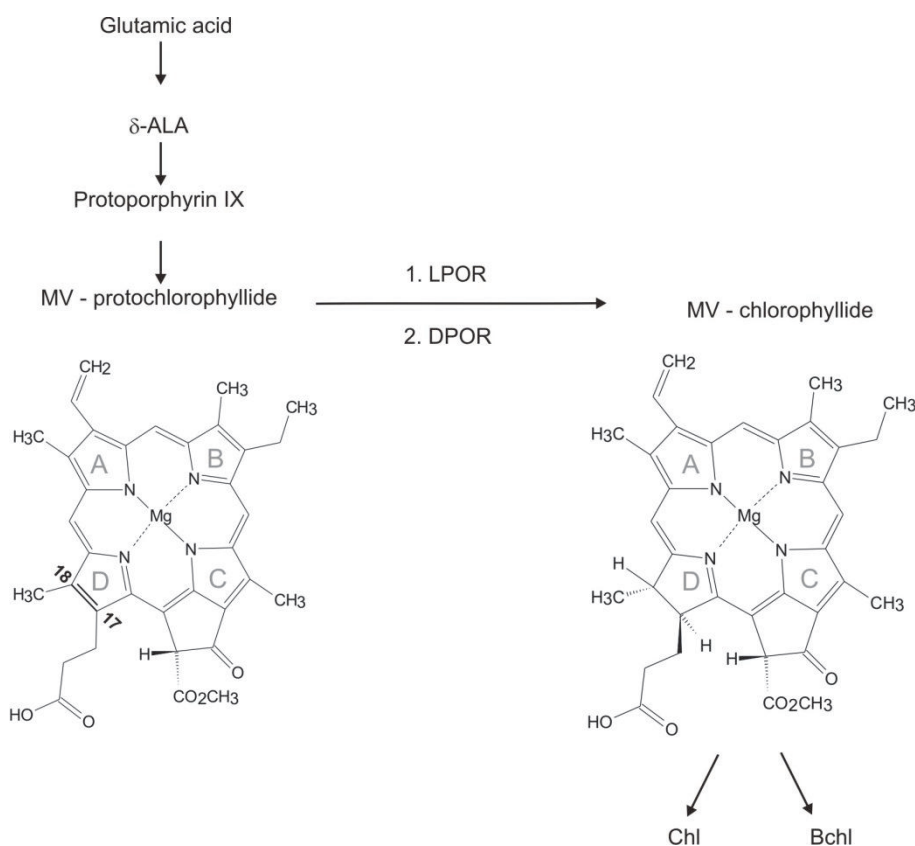


Fig. 1. Outline of the biosynthetic pathway of chlorophyll (Chl) and bacteriochlorophyll (Bchl). Reduction of the C17=C18 double bond in the pyrrole ring D of Pchlde is catalyzed by light-dependent (LPOR) or dark-operative (DPOR) Pchlde oxidoreductases. ALA - aminolevulinic acid, MV - monovinyl.

Table 1. TFT motif sequences used for the data base construction. GI numers and sourse organisms are included. The numbers in bold refer to the position of the first and the last amino acid of TFT motifs.

GI number L subunit of DPOR	Amino acid sequence	Organism
gi 3820555	43 TFTIAGK-----MIPTVVE	59 <i>Heliobacillus mobilis</i>
gi 13878359	43 TFTIAGK-----MIPTVVE	59 <i>Heliobacillus mobilis</i>
gi 226698866	43 TFTIAGR-----MIPTVVE	59 <i>Heliobacterium modesticaldum Ice1</i>
gi 167629377	43 TFTIAGR-----MIPTVVE	59 <i>Heliobacterium modesticaldum Ice1</i>
gi 167592117	43 TFTIAGR-----MIPTVVE	59 <i>Heliobacterium modesticaldum Ice1</i>
gi 41688494	43 TFTLTGS-----LIPTIID	59 <i>Anthoceros formosae</i>
gi 120542	43 TFTLTGF-----LIPTIID	59 <i>Marchantia polymorpha</i>
gi 68052070	43 TFTLTGF-----LIPTIID	59 <i>Huperzia lucidula</i>
gi 182894147	43 TFTLTGF-----LIPTIID	59 <i>Angiopteris evecta</i>
gi 68052162	43 TFTLTGF-----LIPTIID	59 <i>Physcomitrella patens</i> subsp. <i>patens</i>
gi 3913244	43 TFTLTGF-----LIPTIID	59 <i>Picea abies</i>
gi 1168937	43 TFTLTGF-----LIPTIID	59 <i>Pinus thunbergii</i>
gi 120543	43 TFTLTGF-----LIPTIID	59 <i>Pinus contorta</i>
gi 68052192	43 TFTLTGF-----LIPTIID	59 <i>Pinus koraiensis</i>
gi 68052102	43 TFTLTGF-----LIPTIID	59 <i>Larix decidua</i>
gi 172048633	43 TFTLTGF-----LIPTIID	59 <i>Cycas taitungensis</i>
gi 122211814	43 TFTLTGF-----LIPTIID	59 <i>Staurostrum punctulatum</i>
gi 122211735	43 TFTLTGF-----LIPTIID	59 <i>Zygnema circumcarinatum</i>
gi 25008287	43 TFTLTGF-----LIPTIID	59 <i>Chaetosphaeridium globosum</i>
gi 68565046	43 TFTLTGF-----LIPTIID	59 <i>Adiantum capillus-veneris</i>
gi 122224959	43 TFTLTGF-----LIPTIID	59 <i>Chara vulgaris</i>
gi 13878444	43 TFTLTGF-----LIPTIID	59 <i>Mesostigma viride</i>
gi 172045680	43 TFTLTGF-----LIPTIID	59 <i>Chlorokybus atmophyticus</i>
gi 190358902	45 TFTLTGF-----LIPTIID	61 <i>Synechococcus</i> sp. PCC 7002
gi 226706353	45 TFTLTGF-----LIPTIID	61 <i>Microcystis aeruginosa</i> NIES-843
gi 226706352	45 TFTLTGF-----LIPTIID	61 <i>Cyanothece</i> sp. PCC 8801
gi 120545	45 TFTLTGF-----LIPTIID	61 <i>Synechocystis</i> sp. PCC 6803 substr. <i>Kazusa</i>
gi 189082380	43 TFTLTGF-----LIPTIID	59 <i>Acaryochloris marina</i> MBIC11017
gi 120544	43 TFTLTGF-----LIPTIID	59 <i>Leptolyngbya boryana</i>
gi 172046710	43 TFTLTGF-----LIPTIID	59 <i>Anabaena variabilis</i> ATCC 29413
gi 21263466	43 TFTLTGF-----LIPTIID	59 <i>Nostoc</i> sp. PCC 7120
gi 226706354	43 TFTLTGF-----LIPTIID	59 <i>Nostoc punctiforme</i> PCC 73102
gi 123056859	43 TFTLTGF-----LIPTIID	59 <i>Trichodesmium erythraeum</i> IMS101
gi 122194755	43 TFTLTGF-----LIPTIID	59 <i>Pyropia yezoensis</i>
gi 1705819	43 TFTLTGF-----LIPTIID	59 <i>Porphyra purpurea</i>
gi 254813926	43 TFTLTGF-----LIPTIID	59 <i>Cyanothece</i> sp. PCC 7425
gi 172045819	43 TFTLTGF-----LIPTIID	59 <i>Thermosynechococcus elongatus</i> BP-1
gi 81676983	43 TFTLTGF-----LIPTIID	59 <i>Synechococcus elongatus</i> PCC 6301
gi 1705820	43 TFTLTGF-----LIPTIID	59 <i>Synechococcus elongatus</i> PCC 7942
gi 123505315	48 TFTLTGF-----LIPTIID	64 <i>Synechococcus</i> sp. JA-3-3Ab
gi 123502915	48 TFTLTGF-----LIPTIID	64 <i>Synechococcus</i> sp. JA-2-3B'a(2-13)
gi 81709614	43 TFTLTGF-----LIPTIID	59 <i>Gloeobacter violaceus</i> PCC 7421
gi 120541	43 TFTLTGF-----LIPTIID	59 <i>Chlamydomonas reinhardtii</i>
gi 13878446	43 TFALTGF-----LIPTIMD	59 <i>Nephroselmis olivacea</i>
gi 3023485	43 TFTLTGF-----LIPTIID	59 <i>Chlorella vulgaris</i>
gi 68052157	43 TFTLTGF-----LIPTIID	59 <i>Auxenochlorella protothecoides</i>
gi 182894146	43 TFTLTGF-----LIPTIID	59 <i>Leptosira terrestris</i>
gi 122165109	43 TFTLTGF-----LIPTIID	59 <i>Stigeoclonium helveticum</i>
gi 122179518	43 TFTLTGF-----LIPTIID	59 <i>Scenedesmus obliquus</i>
gi 1345782	43 TFTLTGF-----LIPTIID	59 <i>Cyanophora paradoxa</i>
gi 122195140	43 TFTLTGF-----LIPTIID	59 <i>Oltmannsiellopsis viridis</i>
gi 544021	48 TFTLTGF-----LIPTIID	64 <i>Polystichum acrostichoides</i>
gi 254810211	45 TFPLTGH-----LQPTVID	61 <i>Chloroflexus</i> sp. Y-400-fl
gi 13878340	45 TFPLTGH-----LQPTVID	61 <i>Chloroflexus aurantiacus</i> J-10-fl
gi 254810210	45 TFPLTGH-----LQPTVID	61 <i>Chloroflexus aggregans</i> DSM 9485

Table 1 continues on the next page

Table 1 (continued)

GI number L subunit of DPOR	Amino acid sequence		Organism	
gi 189081504	45	TFALTGM-----LQPTVID	61	<i>Roseiflexus castenholzii</i> DSM 13941
gi 166224350	45	TFALTGT-----LQPTVID	61	<i>Roseiflexus</i> sp. RS-1
gi 226698868	45	TFPLTGT-----LQKTVID	61	<i>Prosthecochloris aestuarii</i> DSM 271
gi 226698864	45	TFPLTGT-----LQKTVID	61	<i>Chlorobium phaeobacteroides</i> BS1
gi 226698862	45	TFPITGK-----LQKTVID	61	<i>Chlorobium limicola</i> DSM 245
gi 166224347	45	TFPITGK-----LQKTVID	61	<i>Chlorobium phaeobacteroides</i> DSM 266
gi 189081503	45	TFPITGK-----LQKTVID	61	<i>Chlorobium phaeovibrioides</i> DSM 265
gi 226698867	45	TFPITGK-----LQKTVID	61	<i>Pelodictyon phaeoclathratiforme</i> BU-1
gi 123579265	45	TFPITGK-----LQKTVID	61	<i>Chlorobium chlorochromatii</i> CaD3
gi 123583565	45	TFPITGK-----LQKTVID	61	<i>Chlorobium luteolum</i> DSM 273
gi 226698863	45	TFPITGK-----LQKTVID	61	<i>Chlorobaculum parvum</i> NCIB 8327
gi 13878343	45	TFPITGK-----LQKTVID	61	<i>Chlorobium tepidum</i> TLS
gi 226698865	45	TFPITGH-----LQKTVID	61	<i>Chloroherpeton thalassium</i> ATCC 35110
gi 170652908	76	TFTLTGS-----LVPTVID	92	<i>Dinoroseobacter shibae</i> DFL 12
gi 157913837	76	TFTLTGS-----LVPTVID	92	<i>Dinoroseobacter shibae</i> DFL 12
gi 123066021	76	TFTLTGS-----LVPTVID	92	<i>Roseobacter denitrificans</i> OCh 114
gi 172046597	83	TFTLTGM-----LQPTVID	99	<i>Jannaschia</i> sp. CCS1
gi 114863	79	TFTLTGR-----LQETVID	95	<i>Rhodobacter capsulatus</i>
gi 254810219	74	TFTLTGS-----LVPTVID	90	<i>Rhodobacter sphaeroides</i> KD131
gi 166224348	74	TFTLTGS-----LVPTVID	90	<i>Rhodobacter sphaeroides</i> ATCC 17029
gi 85681290	74	TFTLTGS-----LVPTVID	90	<i>Rhodobacter sphaeroides</i> 2.4.1
gi 225734166	91	TFTLTGS-----LVPTVID	107	<i>Rhodobacter sphaeroides</i> 2.4.1
gi 225734165	91	TFTLTGS-----LVPTVID	107	<i>Rhodobacter sphaeroides</i> 2.4.1
gi 215261299	84	TFTLTGS-----LVPTVID	100	<i>Rhodobacter sphaeroides</i> 2.4.1
gi 215261298	84	TFTLTGS-----LVPTVID	100	<i>Rhodobacter sphaeroides</i> 2.4.1
gi 166224349	74	TFTLTGS-----LVPTVID	90	<i>Rhodobacter sphaeroides</i> ATCC 17025
gi 170652907	78	TFTLTKR-----LVPTVID	94	<i>Bradyrhizobium</i> sp. ORS 278
gi 170652906	78	TFTLTKR-----LVPTVID	94	<i>Bradyrhizobium</i> sp. BTAi1
gi 254810218	80	TFTLTKK-----LVPTVID	96	<i>Rhodospirillum centenum</i> SW
gi 123762521	88	TFTLTKR-----LIPTVID	104	<i>Rhodopseudomonas palustris</i> BisB5
gi 123292175	88	TFTLTKR-----LIPTVID	104	<i>Rhodopseudomonas palustris</i> HaA2
gi 122476964	88	TFTLTKR-----LVPTVID	104	<i>Rhodopseudomonas palustris</i> BisB18
gi 81698290	88	TFTLTKK-----LMPTVID	104	<i>Rhodopseudomonas palustris</i> CGA009
gi 122297133	86	TFTLTKC-----LIPTVID	102	<i>Rhodopseudomonas palustris</i> BisA53
gi 123527299	72	TFTLTKR-----LVPTVID	88	<i>Rhodospirillum rubrum</i> ATCC 11170
gi 13878351	67	TFTLTKR-----LVPTVID	83	<i>Rhodospirillum rubrum</i>
gi 13878348	79	TFTLTKR-----MVPTVID	95	<i>Rubrivivax gelatinosus</i>
gi 254810213	74	TFTLTKR-----LAPTVID	90	<i>Methylobacterium extorquens</i> PA1
gi 254810212	74	TFTLTKR-----LAPTVID	90	<i>Methylobacterium chloromethanicum</i> CM4
gi 254810214	74	TFTLTKR-----LAPTVID	90	<i>Methylobacterium populi</i> BJ001
gi 254810215	74	TFTLTKR-----LAPTVID	90	<i>Methylobacterium radiotolerans</i> JCM 2831
gi 254810216	78	TFTLTKR-----LAPTVID	94	<i>Methylobacterium</i> sp. 4-46
gi 226706355	72	TFTLTHK-----MVPTVID	88	<i>Prochlorococcus marinus</i> str. MIT 9211
gi 81712822	72	TFTLTHK-----MVPTVID	88	<i>Prochlorococcus marinus</i> subsp. <i>marinus</i> str. CCMP1375
gi 182894152	72	TFTLTHK-----MVPTVID	88	<i>Prochlorococcus marinus</i> str. NATL1A
gi 123620280	72	TFTLTHK-----MVPTVID	88	<i>Prochlorococcus marinus</i> str. NATL2A
gi 182894151	72	TFTLTHR-----MVPTVID	88	<i>Prochlorococcus marinus</i> str. MIT 9303
gi 81712691	72	TFTLTHR-----MVPTVID	88	<i>Prochlorococcus marinus</i> str. MIT 9313
gi 182894150	72	TFTLTHK-----MVPTVID	88	<i>Prochlorococcus marinus</i> str. MIT 9301
gi 182894148	72	TFTLTHK-----MVPTVID	88	<i>Prochlorococcus marinus</i> str. AS9601
gi 172047292	72	TFTLTHK-----MVPTVID	88	<i>Prochlorococcus marinus</i> str. MIT 9215
gi 123554484	72	TFTLTHK-----MVPTVID	88	<i>Prochlorococcus marinus</i> str. MIT 9312
gi 182894149	72	TFTLTHK-----MVPTVID	88	<i>Prochlorococcus marinus</i> str. MIT 9515
gi 81712619	72	TFTLTHK-----MVPTVID	88	<i>Prochlorococcus marinus</i> subsp. <i>pastoris</i> str. CCMP1986

Table 1 continues on the next page

Table 1 (continued)

GI number	Amino acid sequence		Organism	
L subunit of DPOR				
gi 123578595	72	TFTLTHK-----MVPTVID	88	<i>Synechococcus</i> sp. CC9605
gi 81574172	72	TFTLTHK-----MVPTVID	88	<i>Synechococcus</i> sp. WH 8102
gi 172047785	72	TFTLTHK-----MVPTVID	88	<i>Synechococcus</i> sp. WH 7803
gi 172046629	72	TFTLTHS-----MVPTVID	88	<i>Synechococcus</i> sp. CC9902
gi 123327701	72	TFTLTHK-----MVPTVID	88	<i>Synechococcus</i> sp. CC9311
gi 172047910	76	TFTLTHK-----MVPTVID	92	<i>Synechococcus</i> sp. RCC307
gi 254810217	79	TFTLTKR-----FVPTVID	95	<i>Methylocella silvestris</i> BL2
gi 170652909	77	TFTLTKR-----LVPTVID	93	<i>Halorhodospira halophila</i> SL1
LPOR				
gi 10720232	182	RFTADGFELSVGTNHLGHFLLTNLLLD	208	<i>Chlamydomonas reinhardtii</i>
gi 1408176	182	RFTADGFELSVGTNHLGHFLLTNLLLD	208	<i>Chlamydomonas reinhardtii</i>
gi 3327258	242	KFSAEGFELSVGTNMGHFLARLLME	268	<i>Marchantia paleacea</i> subsp. <i>diptera</i>
gi 10720231	242	KFSAEGFELSVGTNMGHFLARLLME	268	<i>Marchantia paleacea</i>
gi 15218860	186	SFTAEGFEISVGTNHLGHFLLSRLLLD	212	<i>Arabidopsis thaliana</i>
gi 10720234	186	SFTAEGFEISVGTNHLGHFLLSRLLLD	212	<i>Arabidopsis thaliana</i>
gi 8467964	186	SFTAEGFEISVGTNHLGHFLLSRLLLD	212	<i>Arabidopsis thaliana</i>
gi 79316418	184	SFTAEGFEISVGTNHLGHFLLSRLLLD	210	<i>Arabidopsis thaliana</i>
gi 297843168	186	SFTAEGFELSVGTNHLGHFLLSRLLLD	212	<i>Arabidopsis lyrata</i> subsp. <i>lyrata</i>
gi 297335307	186	SFTAEGFELSVGTNHLGHFLLSRLLLD	212	<i>Arabidopsis lyrata</i> subsp. <i>lyrata</i>
gi 75248671	182	SFTADGFEMSVGVNHLGHFLLARELLA	208	<i>Oryza sativa Japonica</i> Group
gi 115482724	68	SFTADGFEMSVGVNHLGHFLLARELLA	94	<i>Oryza sativa Japonica</i> Group
gi 113639564	68	SFTADGFEMSVGVNHLGHFLLARELLA	94	<i>Oryza sativa Japonica</i> Group
gi 10720236	179	SFTADGFEMSVGVNHLGHFLLARELLE	205	<i>Hordeum vulgare</i>
gi 46019982	155	SYTADGFEMSVGVNHLGHFLLARELLS	181	<i>Zea mays</i>
gi 79325287	185	TYSAEGFELSVATNHLGHFLLARLLLD	211	<i>Arabidopsis thaliana</i>
gi 15234129	185	TYSAEGFELSVATNHLGHFLLARLLLD	211	<i>Arabidopsis thaliana</i>
gi 1583456	185	TYSAEGFELSVATNHLGHFLLARLLLD	211	<i>Arabidopsis thaliana</i>
gi 2507092	185	TYSAEGFELSVATNHLGHFLLARLLLD	211	<i>Arabidopsis thaliana</i>
gi 968977	185	TYSAEGFELSVATNHLGHFLLARLLLD	211	<i>Arabidopsis thaliana</i>
gi 15239574	189	TFTAEGFELSVGINHLGHFLLSRLLID	215	<i>Arabidopsis thaliana</i>
gi 26454645	189	TFTAEGFELSVGINHLGHFLLSRLLID	215	<i>Arabidopsis thaliana</i>
gi 1583455	189	TFTAEGFELSVGINHLGHFLLSRLLID	215	<i>Arabidopsis thaliana</i>
gi 968975	189	TFTAEGFELSVGINHLGHFLLSRLLID	215	<i>Arabidopsis thaliana</i>
gi 79330812	68	TFTAEGFELSVGINHLGHFLLSRLLID	94	<i>Arabidopsis thaliana</i>
gi 10720220	183	TFTAEGFELSVGTNHLGHFLLSRLLLE	209	<i>Cucumis sativus</i>
gi 2244614	183	TFTAEGFELSVGTNHLGHFLLSRLLLE	209	<i>Cucumis sativus</i>
gi 9587209	182	THTADGFELSVGTNHLGHFLLSRLLLE	208	<i>Vigna radiata</i>
gi 10720233	182	TYTADGFELSVGTNHLGHFLLSRLLLD	208	<i>Daucus carota</i>
gi 266742	183	SFTADGFEISVGTNHLGHFLLSRLLLE	209	<i>Pisum sativum</i>
gi 20830	183	SFTADGFEISVGTNHLGHFLLSRLLLE	209	<i>Pisum sativum</i>
gi 227065	171	TFTADGHEMSVGVNHLGHFLLARLLME	197	<i>Hordeum vulgare</i> subsp. <i>vulgare</i>
gi 129708	171	TFTADGHEMSVGVNHLGHFLLARLLME	197	<i>Hordeum vulgare</i>
gi 10720235	171	TFTADGHEMSVGVNHLGHFLLARLLME	197	<i>Triticum aestivum</i>
gi 129707	96	TFTAEGVEMSVGVNHLGHFLLARLLLE	122	<i>Avena sativa</i>
gi 75232717	170	TFTADGYEMSVGVNHLGHFLLARMLD	196	<i>Oryza sativa Japonica</i> Group
gi 115461348	170	TFTADGYEMSVGVNHLGHFLLARMLD	196	<i>Oryza sativa Japonica</i> Group
gi 113565845	170	TFTADGYEMSVGVNHLGHFLLARMLD	196	<i>Oryza sativa Japonica</i> Group
gi 2598163	49	TFTAEGFELSVGTNHLGHFLLSRLLLE	75	<i>Oryza sativa Japonica</i> Group
gi 7330644	184	TYTAEGFELSVGTNHLGHFLLSRLLLE	210	<i>Pinus mugo</i>
gi 226515427	157	TYTKDGFEEVGVTHLGHFLLANMLK	183	<i>Micromonas</i> sp. RCC299
gi 255072981	157	TYTKDGFEEVGVTHLGHFLLANMLK	183	<i>Micromonas</i> sp. RCC299

Statistical analysis included calculation of the number of sequences having a given residue at each position in the sequence with respect to the total number of the sequences in the constructed protein database for LPOR

and BchL/ChL sequences separately. This provided information about the frequency of the occurrence of a given amino acid residue at a certain position in the identified motif.

Modeling of the tertiary structure of LPOR: The tertiary structure of *A. thaliana* PORA (NCBI accession number: NP_200230) was predicted by homology modeling. The modeling templates were identified within PDB deposited proteins and 3 templates with the highest sequence homology to *A. thaliana* PORA were used, *i.e.*,

porcine testicular carbonyl reductase (pdb:1n5d), gluconate 5-dehydrogenase TM0441 *Thermotoga maritima* (pdb: 1vl8) and human carbonyl reductase 3, complexed with NADP⁺ (pdb:2hrb). The modeling was performed by SwissMODEL (Arnold *et al.* 2006) and Modeller 9v8 (John and Šali 2003) for comparison.

Results and discussion

Newly identified amino acid motif in LPOR and the L subunit of DPOR: The comparison of amino acid sequences of *A. thaliana* PORA (NCBI accession number: NP_200230) with BchL/ChlL from the NCBI protein data bank showed a fragment consisting of 14 amino acid residues similar in PORA of *A. thaliana* and all the investigated BchL/ChlL sequences. In the case of *A. thaliana* PORA, the motif (called TFT) showed the following sequence: TFTAEGF-X-LSRLLLD, where -X- was the insert of 13 amino acids not found in the investigated BchL/ChlL sequences (Fig. 2). The identified fragment was then found in all of the investigated plants' LPOR sequences from the NCBI protein data bank. It should be explained that in the search, not only did we focus on finding identical amino acids at a given position in the TFT motif, but we also accepted residues having similar physicochemical character of amino acid side groups.

The summary of amino acid sequence of the TFT motif obtained for the BchL/ChlL and for LPOR sequences is presented in Fig. 3. Threonine and threonine/serine, *i.e.* the amino acids containing hydroxyl group, were found in the 1st position of the TFT motif in all BchL/ChlL and in the majority of LPOR sequences. Arginine or lysine were identified only in four LPOR sequences. Phenylalanine was in 2nd position in all of BchL/ChlL sequences and in 74% of LPOR sequences. In 24% of LPOR sequences, phenylalanine was replaced by tyrosine. Threonine/serine always occurred in the 3rd position in LPOR sequences and in most of BchL/ChlL sequences (85%). In the latter case, apart from threonine, either proline (12 %) or alanine (3%) were identified. In the 4th position, mostly hydrophobic amino acids were found, *i.e.* leucine/isoleucine in BchL/ChlL, and alanine in LPOR sequences. Aspartic or glutamic acids were found in 5th position in all of the LPOR sequences, whereas threonine was detected at this position in 98% of the investigated BchL/ChlL sequences. The next two positions in the TFT motif were more conserved in LPOR, having only glycine in 6th and mostly phenylalanine in 7th position, than in BchL/ChlL in which these two amino acids were also found at respective positions, however, with much lower frequency. The second part of the TFT motif, preceded by the insert in the case of LPOR, started with leucine in 8th position in all the LPOR sequences and in 78 % of BchL/ChlL sequences. The residues in the next three positions (9–11) differed between BchL/ChlL and LPOR (Fig. 3). The positions no. 12 and 13 were occupied by hydrophobic amino

acids, namely, valine or isoleucine in BchL/ChlL and most frequently by leucine in LPOR or less frequently by methionine. Acidic amino acids (aspartic or glutamic) at the last position were found in all the BchL/ChlL sequences, as well as in most of (85%) the LPOR sequences.

Although the TFT motif is not homological between BchL/ChlL and LPOR sequences, the similar physicochemical character of amino acids in respective positions of the motif (in case of LPOR and BchL/ChlL sequences) was observed for 9 out of 14 residues. This provides similar properties of microenvironment created by amino acids of this motif for both oxidoreductases. Assuming a random selection of 14-amino acid length fragment, as well as equal likelihood for each residue in each position of the motif, the probability of the occurrence of an identical motif is 0.2×10^{-7} . The TFT motif contains polar amino acids with hydroxyl groups that can form hydrogen bonds and aromatic residues that are able to interact with the porphyrin ring of Pchlide molecule (Fig. 3). An insert in the TFT motif found in all the investigated LPOR sequences (Fig. 3B) included hydrophilic (S, T), hydrophobic (L, I, V) and aromatic (F, Y) amino acids, as well as histidine. As it can be calculated on the basis of the data shown in Fig. 3B, 54% (*i.e.* 7 from 13) of the residues within LPOR insert were conserved.

The presence of the TFT motif was also checked in SDR proteins and Fe protein of nitrogenase (NifH) using LPOR and BchL/ChlL as a reference, respectively. However, no fragments similar to the TFT motif were observed either in SDR or in NifH sequences (Fig. 2). Therefore, this motif may be involved in the functioning of LPOR and DPOR proteins. Obviously, to find out the physiological role of this motif in two Pchlide reductases, additional experimental data are required. However, among the already published results, some experimental evidence can be found for the significance of the TFT region for LPOR enzymatic activity. For example, Dahlin *et al.* (1999) showed that clustered charge-to-alanine mutagenesis, *i.e.* change of two charged residues to alanines in the DGFE and HLGH motifs of the LPOR sequence resulted in a complete loss of the enzyme activity. The modified fragments corresponded to the positions 5-6-7-1_i and 8-9-10-11_i (Fig. 3) of the TFT motif, respectively. Moreover, inhibition of the LPOR activity was found in the case of mutations of the R or D residues that are localized at the 10th and 14th positions of the TFT motif, respectively.

NifH	- Swiss-Prot P00456 Clostridium pasteurianum	
bchL	- Swiss-Prot P26237 Rhodobacter capsulatus	
PorA	- Swiss-Prot Q42536 Arabidopsis thaliana	
SDR4	- Swiss-Prot Q8WNV7 Sus scrofa	
NifH	-----	
bchL	-----MSPR	4
PorA	MALQAASLVSSAFSVRKDGKLNASASSSFKESSLFGVSLSEQSKADVFSSSLRCKREQSL	60
SDR4	-----	
	<u>GKST</u>	
NifH	-----MRQVAIYCK-GGIGKSTTTQNLTSGLHAM	28
bchL	DDIPDLKGFDDGEGSVQVHDSIEDGLDVGGARVFSVYCK-GGIGKSTSSNLSSAFLSLL	63
PorA	RNNKAIIRAQAIATSTPSVTKSLDRKKTLRKGNVVTGASSGLGLATAKALAETGKWHV	120
SDR4	-----MASTGVERRKPLENKVALVTASTDGIGLAIAARRLAQDGAHV	42
	<u>TGxxxGxG</u>	
NifH	GKTIMVVGCDPKADSTRLLLGGLAQKSVLDTLREEGEDVELDSILKEGYGGIRCVESGGP	88
bchL	GKRVLQIGCDPKHDS-----	78
PorA	IMACRDFLKAERAAQSAGMPKDSYTMHLDLASLDSVRQFVDNFRRAEMPLDVLVCNAAV	180
SDR4	VSSRKQENVDRVTATLQGEGLSVTGTVCHVGKAEDRERLVAMAVNLHGGVDILVS-NAAV	101
	<u>NAA</u>	
NifH	EPGVGCAGRGIIITSINMLEQLGAYTDDLDYVFYDVLGDVCGGFAMPIREGKAQEIIYIVA	148
bchL	-----TFTLTGR-----LQETVIDILKQVNFHPEELRPEDYVTEGFNGV	117
PorA	YQPTANQPTFTAEQFELSVGINHLGHFLLSRLIIDLKNSDYPSKRLIIVGSITGNTNTL	240
SDR4	NPFFGNIIDATEEVWDKILHVNKATVLMTKAVVPEMEKRGGGSVLIVSSVGAYHPPFNL	161
	<u>TFT motif</u>	
NifH	SGEMMALYAANNISKGIQKYAKSGGVRLGGIICNSRKVANNEYELDAFAKELGSQLIHFV	208
bchL	MCVEAGGPPAGTGCGYVVGQTVKLLQHHLLEDTDVVVFDVLGDVCGGFAPLQHADR	177
PorA	AGNVPPKANGLDLRGLAGGLNGLNSSAMIDGGDFVGAKAYKDSKVCNMLTMQEFHRRFHE	300
SDR4	GP-----YNVSKTALLGLTKNLAVELAP	184
	<u>YxxxK</u>	
NifH	PRSPMVTKAEINKQTVIEYDPTCEQAEEYRELARKVDANELFVIPKPMQTQERLEEILMQY	268
bchL	ALIVTANDFDSIYAMNRIIAAVQAKSVNYKVRLAGCVANRSRETNEVDRYCEANFKRIA	237
PorA	DTGITFASLYPGCIATTGLFREHIPLFRTLFPFPQKYITKGYVSESEAGKRLAQVVADPS	360
SDR4	RNIRVNCLAPGLIKTNFSQVLWMDKARKEYMKESLRIRRLGNPEDCAGIVSFLCSEDASY	244
NifH	GLMDL-----	273
bchL	HMPDLDSIRRSRLKKRTLFEEMDDAEDVVMARAEYIRLAETLWRSTGEPGLTPEPLTDRHI	297
PorA	LTKSGVYWSWNKTSASFENQLSQEASDVEKARRVWEVSEKLVGLA-----	405
SDR4	ITGETVVVGGGTASRL-----	260
NifH	-----	
bchL	FELLGFD	304
PorA	-----	
SDR4	-----	

Fig. 2. Protein sequence alignment of NifH from *Clostridium pasteurianum*, BchL from *Rhodobacter capsulatus*, PORA from *Arabidopsis thaliana* and SDR4 (carbonyl reductase) from *Sus scrofa*. In the case of POR and SDR, characteristic motifs: NAA (NADPH-binding) and YxxxK (catalytic) are indicated.

The TFT motif in the homology model of *A. thaliana* PORA: In LPOR sequences (Fig. 2), the TFT motif was found between the NAA motif, which is one of NADPH-binding sites, and the catalytic YxxxK motif (Yang and Cheng 2004). Unfortunately, there are no crystal or NMR structures of LPOR published so far, thus all assumptions need to be made based on homology modeling of known SDR structures. In the present work, we have modeled a representation of the tertiary structure of PORA from *A. thaliana* (NCBI accession number NP_200230) that

has not been modeled until now. There were no significant differences between the models obtained by SwissMODEL and Modeller software in the SDR-homologous regions.

All typical features of SDR (Oppermann *et al.* 2003) were found in the obtained model (Fig. 4A), *i.e.* two long helices are facing a 7-stranded β -sheet and 7 shorter helices. The origin of the TFT motif (*i.e.* T-F-T sequence) was localized on the top of one of the long helices, called α D in the SDR helix numbering (Oppermann *et al.* 2003),

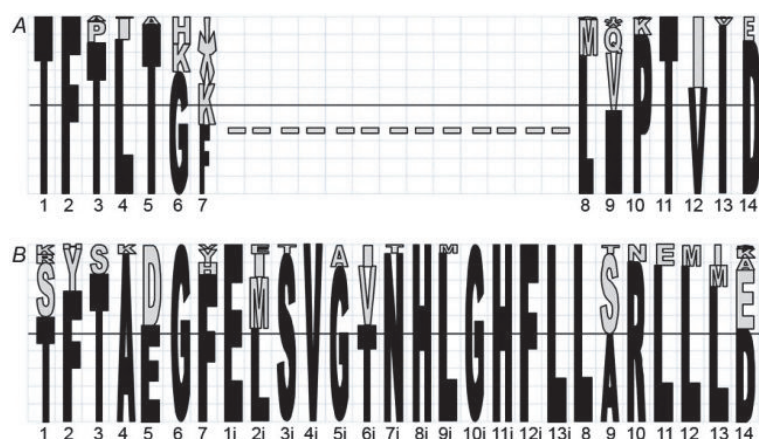


Fig. 3. TFT amino acid motif in Bchl/ChlL (A) and plant LPOR (B). Residues in the insert of LPOR were numbered separately; 'i' stands for insert. Heights of the letters correspond to the frequency of the occurrence of a given amino acid at the given position within the TFT motif calculated for all sequences from each sequence group. The 50% frequency level is marked as the black horizontal line. Asterisk stands for amino acids occurring at a very low frequency.

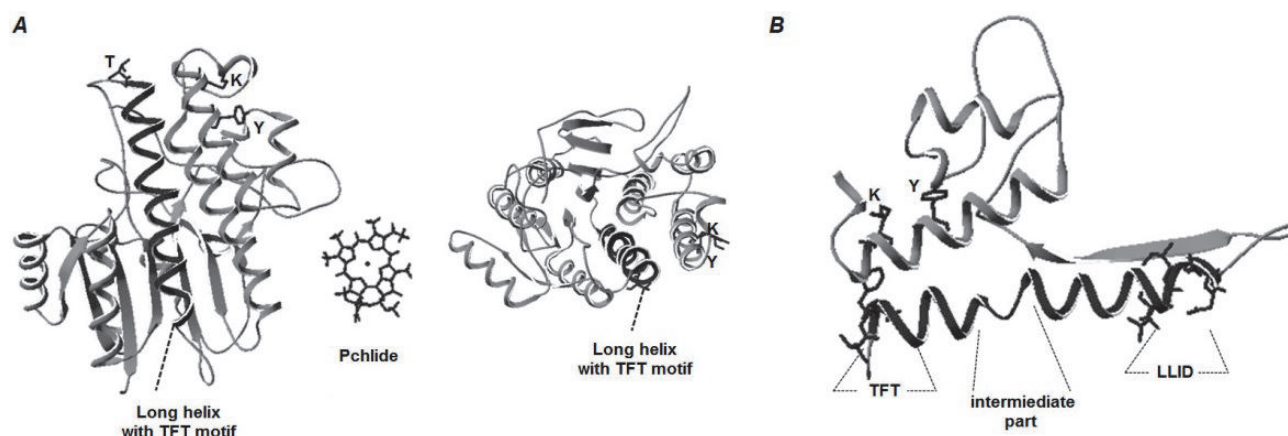


Fig. 4. A: The model of PORA from *Arabidopsis thaliana*: side view (left), top view (right) and Pchlride molecule (middle). The TFT motif was shown as a single helix. Tyrosine and lysine residues are at positions 280 and 284, respectively, corresponding to Y275 and K279 in the catalytic motif (YxxxK) of barley PORB (Lebedev *et al.* 2001) are marked. The estimated distance between the first and the last residues of the motif is 29 Å. For details see the text. B: The fragment of *A. thaliana* LPOR structure, containing the TFT motif with marked T-F-T and L-L-I-D sequences. The internal part of the long helix represents a fragment with a coil structure.

and the whole TFT motif was in this helix. However, the helical structure of this region seems to be forced by the spatial orientation of adjacent elements of the protein structure. When only the fragment of the PORA sequence (90–220 amino acid) was modeled, the central region of the long helix (199–208 amino acid), marked as 'intermediate region' in Fig. 4B, was evidently shown to be an unstructured loop splitting the long helix into two short helices. Using algorithms for protein secondary structure prediction (e.g. GOR4 - Garnier *et al.* 1996, and JUFO - Meiler and Baker 2003), it was also found, with high probability, that these regions are unstructured (not shown).

In the known homology models of LPOR from *Synechocystis* (Townley *et al.* 2001) and barley (Buhr *et al.* 2008), the TFT motif was found within the longest α -helix, like in our model. On the other hand, different conformation of this motif was identified in the 'old' model of pea LPOR (Dahlin *et al.* 1999) where only a part of the TFT motif adopted the helical structure. However, the modeling of the pea LPOR sequence, using the same algorithm that we used for *A. thaliana* LPOR,

gave similar conformation of the TFT motif like that of *A. thaliana* (results not shown). The different structure obtained by Dahlin *et al.* (1999) might have resulted from template selection or from older algorithms introduced into *Modeller 3* and *Modeller 8* softwares than those used in the present work.

In the *Arabidopsis* PORA model, the TFT motif is located in close proximity of the highly conserved Y280 and K284 residues (Fig. 4). This YxxxK motif was shown to be indispensable for catalytic activity of LPOR, where Y residue has been suggested as direct proton donor to C18 during the reduction of Pchlride, and K is supposed to be important in facilitating deprotonation of Y (Wilks and Timko 1995, Lebedev *et al.* 2001, Heyes and Hunter 2002). In the presently modeled conformation, the threonine in 3rd position of the TFT motif faces one of the cysteine residues (Cys-222 in *Synechocystis* POR, which is equivalent to Cys-313 in *A. thaliana* POR), located on the next helix (at the distance of 4 Å). This cysteine is suggested to be protected from oxidation when NADPH is bound (Heyes *et al.* 2000).

It has recently been demonstrated that binding of Pchl_{ide} to LPOR protein occurs *via* strong hydrogen bonds (Sytina *et al.* 2010 and 2011), which was earlier suggested by Solymosi *et al.* (2002). Several fragments of the Pchl_{ide} molecule, involving carbonyl groups and Mg (Fig. 1) may form hydrogen bonds directly or indirectly with methanol molecules (Zhao and Han 2008). Absorption and fluorescence properties of Pchl_{ide} (Mysliwa-Kurdziel *et al.* 2004, 2008), as well as its excited-state relaxation (Dietzek *et al.* 2006, 2009, 2010), were shown to be influenced by its interaction with hydroxyl group-binding solvents. Pchl_{ide} of etioplast inner membranes, where it naturally accumulates during etiolation (Solymosi and Schoefs 2010), showed similar spectroscopic properties to those found in protic solvents (Mysliwa-Kurdziel *et al.* 1999). Another observation worth mentioning is the presence of two highly conservative histidiny residues in the LPOR insert (Fig. 3B), which may provide a coordination site for the Mg of the Pchl_{ide} molecule. Sytina *et al.* (2011) have recently demonstrated hexacoordination of the LPOR-bound Pchl_{ide}.

All of these data indicate the importance of the polarity of the local microenvironment for the excited-state properties of Pchl_{ide}, that are in turn crucial for its photoreduction catalyzed by LPOR. It has not yet been revealed which sites of LPOR molecule participate in the formation of hydrogen-bond network that stabilizes Pchl_{ide} molecule and to what extent hydroxyl group-binding residues of the TFT motif might contribute to this process.

Binding of NADPH to LPOR precedes and probably facilitates Pchl_{ide} binding during assembly of the substrate-enzyme complex and induces conformational changes of LPOR (Heyes and Scrutton 2009; Sytina *et al.* 2008, 2009). These changes influence distances and relative temporary orientation of the single residues of LPOR protein. Interaction of amino acid residues of the TFT motif with Pchl_{ide} molecule is possible, especially when taking into account the helix-loop-helix conformation of the motif (Fig. 4B).

In angiosperms, Pchl_{ide}:LPOR:NADPH complex forms aggregates *in vivo* and it is widely accepted that activity of these ternary complexes is conferred by their aggregation (Schoefs and Franck 2003, Schoefs 2005). Dimerization/oligomerization of LPOR:Pchl_{ide}:NADPH complexes was also demonstrated in some *in vitro* experiments performed on LPOR of angiosperms (Wiktorsson *et al.* 1992, Martin *et al.* 1997, Ouazzani-Chahdi *et al.* 1998). It is still unknown how LPOR monomers are oriented in the dimer/oligomer and which parts of the LPOR molecule participate in the dimerization/oligomerization process. However, it is worth mentioning that long helices are considered to be the main interaction interface in oligomeric SDRs (Filling *et al.* 2002). If so, a possibility to consider is the interaction of two POR monomers with their long helices in head-to-tail orientation.

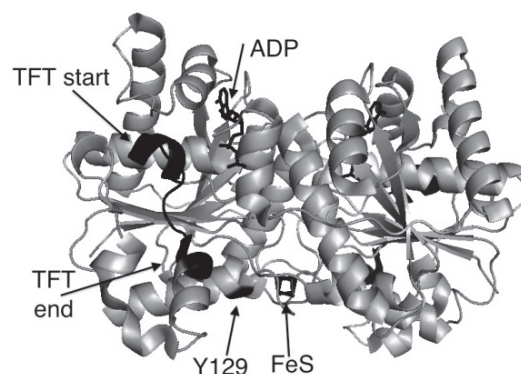


Fig. 5. Crystal structure of L-DPOR from *Rhodospirillum rubrum* (pdb: 3FWY, Sarma *et al.* 2008) with FeS cluster and ADP marked. Tyrosine Y129 is supposed to be important for the interaction between the [BchL]₂ and [BchN-BchB]₂. TFT and TVID correspond to the origin and to the end of TFT motif, respectively. The figure was generated with PyMol (The PyMOL Molecular Graphics System, v. 0.99rc6, Schrödinger, LLC, San Carlos, CA, USA).

The TFT motif in BchL: Concerning the crystal structure of BchL from *Rhodospirillum rubrum* (Sarma *et al.* 2008), the TFT motif can be found in the outer layer of the protein molecule (Fig. 5), close to the tyrosine (*i.e.* Y129), being important for the interaction between the [BchL]₂ and [BchN-BchB]₂ subunits of DPOR. The middle part of the TFT motif is found mostly in the unstructured fragment of the protein, whereas the beginning and the end adopt the helix structure. The recently published crystal structure of the [BchN-BchB]₂ heterotetramer from *Rhodospirillum rubrum* (Muraki *et al.* 2010) revealed that Pchl_{ide} is bound on the interface of heterotetramer consisting of two catalytic [BchN-BchB] heterodimers, in a cavity formed by hydrophobic amino acids, without any involvement of the BchL in the process. Nevertheless, the C-terminal fragment of BchB, which is well conserved and probably important for Pchl_{ide} reduction, remains unresolved in the obtained structure and was described as disordered (Muraki *et al.* 2010).

On the other hand, biochemical studies showed that the interaction between the L-protein and the catalytic NB-protein was essential for Pchl_{ide} reduction (Nomata *et al.* 2008, Bröcker *et al.* 2008, Wätzlich *et al.* 2009). Binding of Pchl_{ide} to the NB-protein was required for the whole DPOR complex formation (Bröcker *et al.* 2010b). It was recently shown that this binding was the initial step of DPOR catalysis, which promotes docking of the L-protein to the NB-protein, and is followed by ATP hydrolysis and Pchl_{ide} reduction (Bröcker *et al.* 2008, 2010b).

Even though the catalytic mechanism of DPOR has been proposed and the crystal structure of DPOR subunits has been resolved, the structure and the molecular mechanism of the assembly of the whole DPOR complex have not been elucidated until now. In particular, the mechanism of docking of [BchL]₂ dimer to [BchN-BchB]₂



Fig. 6. Glycine-rich motif of LPOR (A), SDR (B), L subunit of DPOR (C) and NifH (D). Heights of the letters correspond to the frequency of the occurrence of a given amino acid at the given position within the glycine-rich motif calculated for all sequences from each sequence group. The 50% frequency level is marked as the black horizontal line. Asterisks stand for amino acids occurring at very low frequency. The analysis was performed on protein sequences found in NCBI.

heterotetramer and that of Pchlide (and Chlide)-enzyme interactions in DPOR complex still need detailed investigation. With the currently available data, one can only speculate that the TFT motif may play a role in docking of the L-protein to the NB-protein, for example by interacting with Pchlide molecule already bound to the

BchN-BchB dimer. Pchlide might occur in the cavity formed by the BchN-BchB dimer and BchL- interface if we allow the possibility of different docking of the L-protein as opposed to the one proposed on the basis of the comparison with the nitrogenase enzyme complex. Sarma *et al.* (2008) have noticed some structural differences between the docking surface of the NifH and the respective fragments of BchL. It has to be taken into consideration that, although the homology between nitrogenase and DPOR is high, their substrates are completely different. Bröcker *et al.* (2010a) have also suggested that the common ancestor of DPOR and nitrogenase is an unknown nitrogenase-like protein.

Glycine-rich motif: Both LPOR and the BchL/ChlL subunits of DPOR are able to bind NADPH and ATP, respectively, that is important for their catalytic activity. In the case of LPOR, the presence of the conserved NADPH binding motif, *i.e.* GxxxGxG, was one of the reasons for their classification as an SDR protein (Wilks and Timko 1995). Our investigation showed 100% homology for all the residues of the motif in the investigated LPOR sequences (Fig. 6A), meaning that it was more conserved than those described for SDR proteins (Fig. 6B). The highly conserved glycine-rich motif YGKGGIGKST (Fig. 6C,D) that is involved in ATP binding by the BchL of DPOR and NifH of nitrogenase, resembles GxGxxG motif characteristic for the dinucleotide-binding motif found in the family of medium-chain dehydrogenases/reductases (Benach *et al.* 2001). The occurrence of glycine rich motifs both in the L subunit of DPOR and in LPOR is an example of a wider convergence resulting from specific physicochemical and steric demands of the nucleotide-binding site.

Conclusions: In the present paper, we have identified the fragment of amino acid sequence, called TFT motif, having similar physicochemical properties in LPOR and in the L subunit of DPOR proteins. We have indicated a possible significance of this motif with regard to some known facts about LPOR and DPOR proteins. The current findings are important for the following future investigations: (1) mutagenesis experiments on the function of specific amino acids and (2) biochemical and biophysical studies aimed at revealing the molecular mechanism of the assembly of DPOR complex, as well as LPOR aggregation in prolamellar bodies. Moreover, it was interesting to show similarity of the two oxidoreductases generally regarded as completely unrelated. This observation may be important in detailed elucidation of the evolutionary origin of the two different protochlorophyllide oxidoreductases.

References

- Arnold, K., Bordoli, L., Kopp, J., Schwede, T.: The SWISS-MODEL workspace: A web-based environment for protein structure homology modeling. – *Bioinformatics* **22**: 195-201, 2006.
- Belyaeva, O.B., Litvin, F.F.: Photoactive pigment–enzyme complexes of chlorophyll precursor in plant leaves. – *Biochemistry Moscow* **72**: 1458-1477, 2007.
- Benach, J., Atrian, S., Ladenstein, R., González-Duarte, R.: Genesis of *Drosophila* ADH: the shaping of the enzymatic activity from a SDR ancestor. – *Chem-Biol Interactions* **130-132**: 405-415, 2001.
- Bröcker, M.J., Schomburg, S., Heinz, D.W., Jahn, D., Schubert, W.D., Moser, J.: Crystal structure of the nitrogenase-like dark operative protochlorophyllide oxidoreductase catalytic complex (ChlN/ChlB)₂. – *J. Biol. Chem.* **285**: 27336-27345, 2010a.
- Bröcker, M.J., Virus, S., Ganskow, S., Heathcote, P., Heinz, D.W., Schubert, W.D., Jahn, D., Moser, J.: ATP-driven reduction by dark-operative protochlorophyllide oxidoreductase from *Chlorobium tepidum* mechanistically resembles nitrogenase catalysis. – *J. Biol. Chem.* **283**: 10559-10567, 2008.
- Bröcker, M.J., Wätzlich, D., Saggi, M., Lenzian, F., Moser, J., Jahn, D.: Biosynthesis of (Bacterio)chlorophylls. ATP-dependent transient subunit interaction and electron transfer of dark operative protochlorophyllide oxidoreductase. – *J. Biol. Chem.* **285**: 8268-8277, 2010b.
- Buhr, F., El Bakkouri, M., Valdez, O., Pollmann, S., Lebedev, N., Reinbothe, S., Reinbothe, C.: Photoprotective role of NADPH:protochlorophyllide oxidoreductase A. – *Proc. Nat. Acad. Sci. USA* **105**: 12629-12634, 2008.
- Dahlin, C., Aronsson, H., Wilks, H., Lebedev, N., Sundqvist, C., Timko, M.P.: The role of protein surface charge in catalytic activity and chloroplast membrane association of the pea NADPH: protochlorophyllide oxidoreductase (POR) as revealed by alanine scanning mutagenesis. – *Plant Mol. Biol.* **39**: 309-323, 1999.
- Dietzek, B., Kiefer, W., Popp, J., Hermann, G., Schmitt, M.: Solvent effects on the excited-state processes of protochlorophyllide: A femtosecond time-resolved absorption study. – *J. Phys. Chem.* **110**: 4399-4406, 2006.
- Dietzek, B., Tschierlei, S., Hermann, G., Yartsev, A., Pascher, T., Sundstrom, V., Schmitt, M., Popp, J.: Protochlorophyllide *a*: a comprehensive photophysical picture. – *Chem. Phys. Phys. Chem.* **10**: 144-150, 2009.
- Dietzek, B., Tschierlei, S., Hanf, R., Seidel, S., Yartsev, A., Schmitt, M., Hermann, G., Popp, J.: Dynamics of charge separation in the excited-state chemistry of protochlorophyllide. – *Chem. Phys. Lett.* **492**: 157-163, 2010.
- Filling, C., Berndt, K.D., Benach, J., Knapp, S., Prozorowski, T., Nordling, E., Ladenstein, R., Jörnvall, H., Oppermann, U.: Critical residues for structure and catalysis in short-chain dehydrogenases/reductases. – *J. Biol. Chem.* **277**: 25677-25684, 2002.
- Garnier, J., Gibrat, J.F., Robson, B.: GOR method for predicting protein secondary structure from amino acid sequence. – In: Doolittle, R.F. (ed.): *Methods in Enzymology* **266**: 540-553, 1996.
- Heyes, D.J., Hunter, C.N.: Site-directed mutagenesis of Tyr-189 and Lys-193 in NADPH: protochlorophyllide oxidoreductase from *Synechocystis*. – *Biochem. Soc. Trans.* **30**: 601-604, 2002.
- Heyes, D.J., Hunter, C.N.: Making light work of enzyme catalysis: protochlorophyllide oxidoreductase. – *Trends Plant Sci.* **30**: 642-649, 2005.
- Heyes, D.J., Martin, G.E., Reid, R.J., Hunter, C.N., Wilks, H.M.: NADPH:protochlorophyllide oxidoreductase from *Synechocystis*: overexpression, purification and preliminary characterisation. – *FEBS Lett.* **483**: 47-51, 2000.
- Heyes, D.J., Scrutton, N.S.: Conformational changes in the catalytic cycle of protochlorophyllide oxidoreductase: what lessons can be learnt from dihydrofolate reductase? – *Biochem. Soc. Trans.* **37**: 354-357, 2009.
- Igarashi, R.Y., Seefeldt, L.C.: Nitrogen fixation: the mechanism of the Mo-dependent nitrogenase. – *Crit. Rev. Biochem. Mol. Biol.* **38**: 351-381, 2003.
- John, B., Šali, A.: Comparative protein structure modeling by iterative alignment, model building and model assessment. – *Nucl. Acids Res.* **31**: 3982-3992, 2003.
- Lebedev, N., Karginova, O., McIvor, W., Timko, M.P.: Tyr275 and Lys279 stabilize NADPH within the catalytic site of NADPH:protochlorophyllide oxidoreductase and are involved in the formation of the enzyme photoactive state. – *Biochemistry* **40**: 12562-12574, 2001.
- Martin, G.E., Timko, M.P., Wilks, H.M.: Purification and kinetic analysis of pea (*Pisum sativum* L.) NADPH:protochlorophyllide oxidoreductase expressed as a fusion with maltose-binding protein in *Escherichia coli*. – *Biochem. J.* **325**: 139-145, 1997.
- Masuda, T.: Recent overview of the Mg branch of the tetrapyrrole biosynthesis leading to chlorophylls. – *Photosynth. Res.* **96**: 121-143, 2008.
- Meiler, J., Baker, D.: Coupled prediction of protein secondary and tertiary structure. – *Proc. Nat. Acad. Sci. USA* **100**: 12105-12110, 2003.
- Muraki, N., Nomata, J., Ebata, K., Mizoguchi, T., Shiba, T., Tamiaki, H., Kurisu, G., Fujita, Y.: X-ray crystal structure of the light-independent protochlorophyllide reductase. – *Nature* **465**: 110-114, 2010.
- Mysliwa-Kurdziel, B., Franck, F., Strzałka, K.: Analysis of fluorescence lifetime of protochlorophyllide and chlorophyllide in isolated etioplast membranes measured from multifrequency cross-correlation phase fluorometry. – *Photochem. Photobiol.* **70**: 616-623, 1999.
- Mysliwa-Kurdziel, B., Kruk, J., Strzałka, K.: Fluorescence lifetimes and spectral properties of protochlorophyllide in organic solvents and their relations to the respective parameters in vivo. – *Photochem. Photobiol.* **79**: 62-67, 2004.
- Mysliwa-Kurdziel, B., Solymosi, K., Kruk, J., Böddi, B., Strzałka, K.: Solvent effects on fluorescence properties of protochlorophyll and its derivatives with various porphyrin side chains. – *Eur. Biophys. J.* **37**: 1185-1193, 2008.
- Nomata, J., Ogawa, T., Kitashima, M., Inoue, K., Fujita, Y.: NB-protein (BchN–BchB) of dark-operative protochlorophyllide reductase is the catalytic component containing oxygen-tolerant Fe–S clusters. – *FEBS Lett.* **582**: 1346-1350, 2008.
- Oppermann, U., Filling, C., Hult, M. *et al.*: Short-chain dehydrogenases/reductases (SDR): the 2002 update. – *Chem-Biol. Interactions* **143/144**: 247-253, 2003.

- Ouazzani-Chahdi, M.A., Schoefs, B., Franck, F.: Isolation and characterization of photoactive complexes of NADPH:protochlorophyllide oxidoreductase from wheat. – *Planta* **206**: 673-680, 1998.
- Pruitt, K.D., Tatusova, T., Maglott, D.R.: NCBI reference sequences (RefSeq): a curated non-redundant sequence database of genomes, transcripts and proteins. – *Nucl. Acids Res.* **35**: D61–D65, 2006.
- Reinbothe, C., El Bakkouri, M., Buhr, F., Muraki, N., Nomata, J., Kurisu, G., Fujita, Y., Reinbothe, S.: Chlorophyll biosynthesis: spotlight on protochlorophyllide reduction. – *Trends Plant Sci.* **15**: 614-624, 2010.
- Sarma, R., Barney, B.M., Hamilton, T.L., Jones, A., Seefeldt, L.C., Peters, J.W.: Crystal structure of the L protein of *Rhodospira rubra* light-independent protochlorophyllide reductase with MgADP bound: a homologue of the nitrogenase Fe protein. – *Biochemistry* **47**: 13004-13015, 2008.
- Schoefs, B.: Protochlorophyllide reduction – what is new in 2005? – *Photosynthetica* **43**: 329-343, 2005.
- Schoefs, B., Franck, F.: Protochlorophyllide reduction: mechanisms and evolution. – *Photochem. Photobiol.* **78**: 543-557, 2003.
- Solymosi, K., Schoefs, B.: Etioplast and etio-chloroplast formation under natural conditions: the dark side of chlorophyll biosynthesis in angiosperms. – *Photosynth. Res.* **105**: 143-166, 2010.
- Solymosi, K., Smeller, L., Böddi, B., Fidy, J.: Activation volumes of processes linked to the phototransformation of protochlorophyllide determined by fluorescence spectroscopy at high pressure. – *Biochim. Biophys. Acta* **1554**: 1-4, 2002.
- Sytina, O.A., Alexandre, M.T., Heyes, D.J., Hunter, C.N., Robert, B., van Grondelle, R., Groot, M.L.: Enzyme activation and catalysis: characterisation of the vibrational modes of substrate and product in protochlorophyllide oxidoreductase. – *Phys. Chem. Chem. Phys.* **13**: 2307-2313, 2011.
- Sytina, O.A., Heyes, D.J., Hunter, C.N., Alexandre, M.T., van Stokkum, I.H.M., van Grondelle, R., Groot, M.L.: Conformational changes in an ultrafast light-driven enzyme determine catalytic activity. – *Nature* **456**: 1001-1004, 2008.
- Sytina, O.A., Heyes, D.J., Hunter, C.N., Groot, M.L.: Ultrafast catalytic processes and conformational changes in the light-driven enzyme protochlorophyllide oxidoreductase (POR). – *Biochem. Soc. Trans.* **37**: 387-391, 2009.
- Sytina, O.A., van Stokkum, I.H.M., Heyes, D.J., Hunter, C.N., van Grondelle, R., Groot, M.L.: Protochlorophyllide excited-state dynamics in organic solvents studied by time-resolved visible and mid-infrared spectroscopy. – *J. Phys. Chem.* **114**: 4335-4344, 2010.
- Thompson, J.D., Higgins, D.G., Gibson, T.J.: CLUSTAL W: improving the sensitivity of progressive multiple sequence alignment through sequence weighting, position-specific gap penalties and weight matrix choice. – *Nucl. Acids Res.* **22**: 4673-4680, 1994.
- Townley, H.E., Sessions, R.B., Clarke, A.R., Dafforn, T.R., Griffiths, W.T.: Protochlorophyllide oxidoreductase: a homology model examined by site directed mutagenesis. – *Proteins* **44**: 329-335, 2001.
- Wätzlich, D., Bröcker, M.J., Uliczka, F., Ribbe, M., Virus, S., Jahn, D., Moser, J.: Chimeric nitrogenase-like enzymes of (bacterio)chlorophyll biosynthesis. – *J. Biol. Chem.* **284**: 15530-15540, 2009.
- Wiktorsson, B., Ryberg, M., Gough, S., Sundqvist, C.: Isoelectric focusing of pigment-protein complexes solubilized from non-irradiated and irradiated prolamellar bodies. – *Physiol. Plant.* **82**: 659-669, 1992.
- Wilks, H.M., Timko, M.P.: A light-dependent complementation system for analysis of NADPH:protochlorophyllide oxidoreductase: Identification and mutagenesis of two conserved residues that are essential for enzyme activity. – *Proc. Nat. Acad. Sci. USA* **92**: 724-728, 1995.
- Yang, J., Cheng, Q.: Origin and evolution of the light-dependent protochlorophyllide oxidoreductase (LPOR) genes. – *Plant Biol.* **6**: 537-544, 2004.
- Zhao, G.J., Han, K.L.: Site-specific solvation of the photo-excited protochlorophyllide a in methanol: formation of the hydrogen-bonded intermediate state induced by hydrogen bond strengthening. – *Biophys. J.* **94**: 38-46, 2008.